E3S Web of Conferences **475**, 03002 (2024) https://doi.org/10.1051/e3sconf/202447503002
InCASST 2023

Numerical investigation on the effect of blunt body deflector on darieus turbine performance

Ahmad Syafiq Rofi'i[1], *Aditia* Aulia[1*], *Muhammad Ferry* Fadri[1], *Muhammad Haidar* Syarif[1], *Elvira Rosmawati* Rahman[1], and *Gunawan Dwi* Haryadi[2]

[1]Department of Mechanical Engineering, Republic of Indonesia Defense University, IPSC Area, Sentul, Bogor, Indonesia
[2]Department of Mechanical Engineering, Diponegoro University, Semarang, Indonesia

Abstract. One of the renewable energy source that is abundant but has not been used optimally is wind energy. Roads are currently the main transportation infrastructure along with the increasing number of motorized vehicles. Wind is one of the best renewable energy sources that can be utilized on the highway where it can be used as a power source to drive the Vertical Axis Wind Turbine (VAWT). Darrieus type turbines can operate at low wind speeds and do not require a specific wind direction. However, the installation of this wind turbine on the highway can be hampered due to the presence of highway light poles. We simulate a light pole as a blunt object placed in front of the turbine which will then be observed for the ratio of torque produced to compare the performance of the turbine with a blunt body and without a blunt body. This study aims to determine the effect of the diameter ratio and distance between the turbine and the blunt object on the torque generated on the rotor. This research uses CFD simulation on NACA 4415 foil. The results showed that placing a blunt object in front of the Darrieus turbine increased the turbine torque. The most optimal increase in torque is obtained at a distance of 700 mm with a blunt body diameter of 0.6 DT or 0.3 DT which can increase the torque output of the turbine.

1 Introduction

Road transportation has been the primary transport method in Indonesia. Roads have been a crucial element in connecting rural and urban areas. Road transport is considered the most reliable means of transport in the country, as other means of transport such as railroads have not yet fully developed and are only available in big cities, and the country relies heavily on passenger vehicles. Based on the data from the national statistics center, the total number of motor vehicles increased from 105,303,318 vehicles in 2015 to 141,992,573 vehicles in 2021 [1] and these numbers are expected to increase in the following years. The exact type of vehicles as well as their quantity can be seen in the table 1 below.

* Corresponding author: aditya.aulia@idu.ac.id

© The Authors, published by EDP Sciences. This is an open access article distributed under the terms of the Creative Commons Attribution License 4.0 (https://creativecommons.org/licenses/by/4.0/).

 https://doi.org/10.1051/e3sconf/202447503002

Table 1. Vehicle type and quantity in Indonesia from 2015-2021. Data taken from BPS (https://www.bps.go.id/indicator/17/57/2/perkembangan-jumlah-kendaraan-bermotor-menurut-jenis.html, accesed on 14 August 2023)

Motor Vehicle Type	Vehicle Quantity						
	2015	**2016**	**2017**	**2018**	**2019**	**2020**	**2021**
Passenger Car	12 304 221	13 142 958	13 968 202	14 830 698	15 592 419	15 797 746	16 413 348
Passenger Bus	196 309	204 512	213 359	222 872	231 569	233 261	237 566
Freight Car	4 145 857	4 326 731	4 540 902	4 797 254	5 021 888	5 083 405	5 299 361
Motorcycle	88 656 931	94 531 510	100 200 245	106 657 952	112 771 136	115 023 039	120 042 298
Total	**105 303 318**	**112 205 711**	**118 922 708**	**126 508 776**	**133 617 012**	**136 137 451**	**141 992 573**

This growth of motor vehicles means an increased need for roadways, specifically highways. According to the Ministry of Public Works and Public Housing, the government had built 2,832 km of operational highways by the end of 2022. This number is expected to increase to 4,761 km by 2024. These roads needed power to operate their lights and traffic signs. However, using regular fuel power plants to power these roads is less economical in the long run [2]. Thus, these roads need to be able to sustain itself. One possible means of achieving this is by using a wind turbine installed on the road's divider where it would be spun by passing vehicles. In this research, Vertical Axis Wind Turbine (VAWT) is used. This turbine configuration is chosen due to the relatively low wind velocity of the passing vehicles which produces an average wind speed of 4.4 m/s [3]. VAWT only required a minimum wind speed of 2 m/s compared to its Horizontal Axis Wind Turbine (HAWT) counterpart which needed a minimum wind velocity of 6 m/s [4]. Other advantages of the VAWT configuration are lower noise and less required space, making it suitable for urban applications [4]. The VAWT configuration is also favorable for use on highways as it can pick up wind from both sides (left and right) when installed on the road divider [5]. However, the installation of the turbine may be hampered by highway light poles that can affect the performance of the turbine. This paper aims to investigate the effect of highway light poles on the turbine's performance. CFD software will be used to simulate the poles' effect on the turbine. The light pole will be simulated as a blunt body object placed in front of the turbine. The resulting torque of the turbine with the blunt body will be compared to the turbine's performance with no blunt body.

2 Methods and procedures

This study relied on the use of CFD software. Specifically, SolidWorks Flow Simulation was chosen to conduct the necessary calculations. This approach is commonly used as a way to reduce the risk of failure and minimize expenses before carrying out actual experiments. Additionally, in certain situations, simulations can actually serve as a replacement for experiments, especially when dealing with particularly intricate models.

Solidworks Flow Simulation Use Navier-Stokes Equation to solve the flow problem [6]. Navier Stokes equation is a formulation of mass, momentum, and energy conservation.

$$\frac{\partial \rho}{\partial t} + \frac{\partial(\rho u_i)}{\partial x_i} = 0 \tag{1}$$

$$\frac{\partial(\rho u_i)}{\partial t} + \frac{\partial}{\partial x_j}(\rho u_i u_j) + \frac{\partial P}{\partial x_i} = \frac{\partial}{\partial x_j}\left(\tau_{ij} + {\tau_{ij}}^R\right) + S_i \tag{2}$$

$$\frac{\partial \rho H}{\partial t} + \frac{\partial \rho u_i H}{\partial x_i} = \frac{\partial}{\partial x_j}\left(u_j\left(\tau_{ij} + {\tau_{ij}}^R\right) + q_i\right) + \frac{\partial p}{\partial t} - {\tau_{ij}}^R \frac{\partial u_i}{\partial x_j} + \rho\varepsilon + S_i u_i + Q_H \tag{3}$$

$$H = h + \frac{u^2}{2} \tag{4}$$

SolidWorks Flow Simulation utilizes the modified k-ε model for turbulence prediction. The aim of this model is to simplify the prediction of turbulence. The modified k-ε model explains the behavior of homogeneous fluids with turbulent, laminar, and transitional flows. It takes into account the conservation laws of turbulence.

$$\frac{\partial \rho k}{\partial t} + \frac{\partial \rho k u_i}{\partial x_i} = \frac{\partial}{\partial x_i}\left(\left(\mu + \frac{\mu_t}{\sigma_k}\right)\frac{\partial k}{\partial x_i}\right) + \tau_{ij}{}^R \frac{\partial u_i}{\partial x_j} - \rho\varepsilon + \mu_i P_B \quad (5)$$

$$\frac{\partial \rho \varepsilon}{\partial t} + \frac{\partial \rho \varepsilon u_i}{\partial x_i} = \frac{\partial}{\partial x_i}\left(\left(\mu + \frac{\mu_i}{\sigma_i}\right)\frac{\partial k}{\partial x_i}\right) + C_{\varepsilon 1}\frac{\varepsilon}{k}\left(f_1 \tau_{ij}{}^R \frac{\partial u_i}{\partial x_j} + C_B \mu_t P_B\right) - f_2 C_{\varepsilon 2}\frac{\rho \varepsilon^2}{k} \quad (6)$$

$$\tau_{ij} = \mu S_{ij}, \tau_{ij}{}^R = \mu_i S_{ij} - \frac{2}{3}\rho k \delta_{ij}, S_{ij} = \frac{\partial u_i}{\partial x_j} + \frac{\partial u_j}{\partial x_i} - \frac{2}{3}\delta_{ij}\frac{\partial u_k}{\partial x_k}, \quad (7)$$

$$P_B = -\frac{g_i}{\sigma_B}\frac{1}{\rho}\frac{\partial \rho}{\partial x_i} \quad (8)$$

Where $-\rho uj\ '\ ui\ '$ is the Reynolds stress model, ui is the velocity component, P is fluid pressure, ρ is fluid density, τ is deviatoric stress tensor, ε is the dissipation of turbulent kinetic energy, k is turbulent kinetic energy, h is enthalpy, μ is dynamic viscosity of fluid, μ_t is eddy viscosity, Q_H is the amount of heat, and S is entropy

The aim of this simulation is to investigate the effect caused by highway light poles considered as a blunt body in front of the turbine shown in Figure 1.

This simulation involves the use of the NACA 4415 airfoil, with a blunt body positioned in front of the turbine at varying x-axis distance between 700 mm and 1600 mm with 100 mm increment. The diameter of the blunt body ranges from 0.1 times turbine diameter DT to 1 times DT. The inlet acts as a velocity inlet, with an approximate velocity of 4.4 m/s. This velocity is based on the data from Nassir et al. The outlet functions as a wind outlet with a pressure of 101325 Pa. A schematic of this configuration is shown in Figure 2.

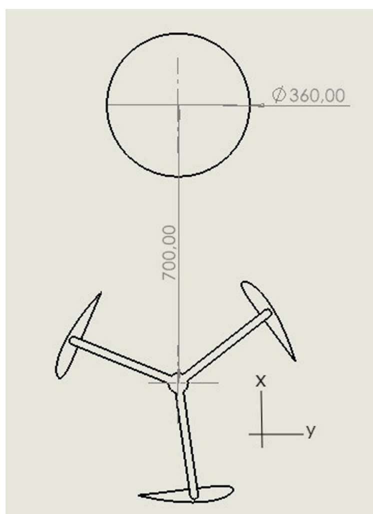

Fig. 1. Simulation setup with blunt body.

 https://doi.org/10.1051/e3sconf/202447503002

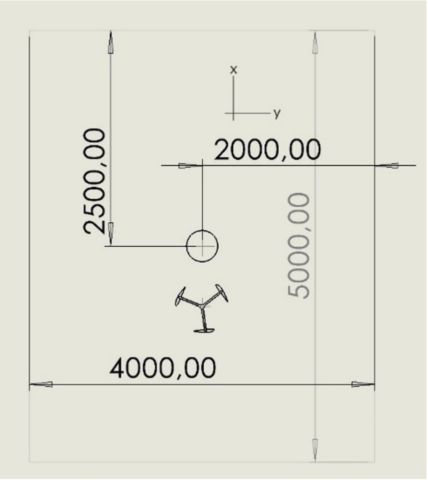

Fig. 2. Boundary condition setup.

The SolidWorks Flow Simulation uses an immersed body mesh approach, which consists of rectangular cells adjacent to each other and to the external boundary of the computational domain. The mesh creation process is independent of geometry and the cells can intersect the boundary between solid and fluid as needed. This Cartesian-based mesh approach offers several advantages such as simplicity, speed, and robustness of the mesh generation algorithm, minimal local truncation errors, and robustness of the differential schemes [6]. The mesh domain of the simulation is shown in Figure 3.

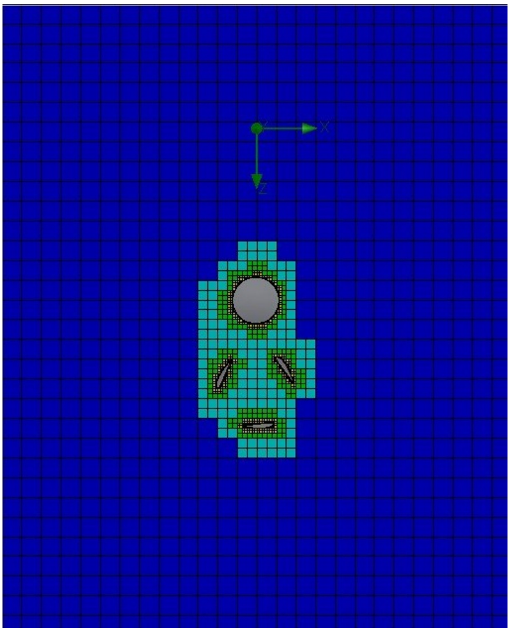

Fig. 3. Simulation meshing.

To achieve precise results with limited computational resources, a specific type of mesh is used. An automatic global meshing method was used to conduct multiple simulations efficiently, with a level 6 mesh and level 4 refinement for local meshing. This approach allowed for collecting highly accurate data while maximizing the available resources.

3 Result and discussion

The simulation is performed by varying the x-axis distance with 100 mm increment from 700 mm to 1600 mm, while for every 100 mm the blunt body diameter is varied from 0,1 times DT to 1 times DT in 0,1 times DT increment.

The torque produced by the turbine, as depicted in Figure 5, reveals a noteworthy trend. It is evident from the data that the presence of a blunt body placed in front of the turbine leads to a decrease in torque production. This decrease is particularly pronounced as the distance between the blunt body and the turbine increases. In other words, the further the blunt body is positioned in front of the turbine, the more significant the reduction in torque output. This finding highlights the crucial relationship between the placement of the blunt body and the resulting torque, suggesting that the placement of the turbine from such obstructions has a significant impact on the turbine’s performance.

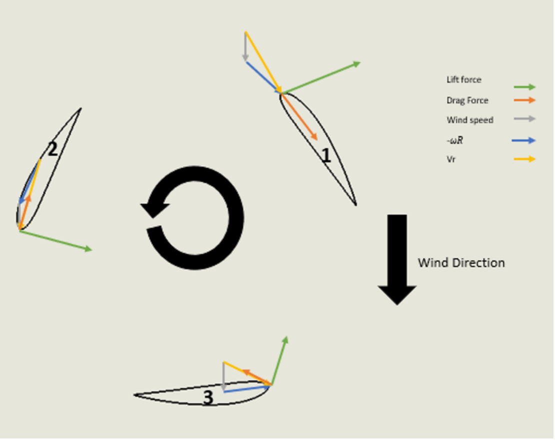

Fig. 4. Schematic of force diagram acting on the turbine blades.

The rotation of the Daeriuss turbine is primarily achieved through the utilization of lift force, which is a pivotal component in its operation. In addition to the lift force, each blade of the turbine incorporates an airfoil design that inevitably generates a complementary drag force. A visual representation of the forces acting upon the turbine can be found in Figure 4, providing valuable insights into its dynamic performance characteristics. Upon closer examination of Figure 4, it becomes evident that blade number 1 contributes negatively to the overall torque generated by the turbine, effectively resisting its rotation. In stark contrast, turbine blades numbered 2 and 3 exert a positive torque, actively propelling the turbine's rotation. An intriguing facet emerges as we delve deeper into this dynamic interplay between forces and torques: the magnitude of torque generated by these blades exhibits a direct correlation with the prevailing wind velocity. Specifically, higher wind speeds correspond to increased torque production by blades 2 and 3, amplifying the turbine's rotational power. Conversely, for blade number 1, this relationship is inverse, resulting in diminished torque production as wind velocity escalates.

Understanding the intricate mechanics of the Daeriuss turbine's operation requires an appreciation of the dual forces at work – lift and drag. The lift force serves as the primary driver behind the turbine's rotation, harnessed through the airfoil-shaped blades. However, it is essential to acknowledge the presence of drag force as well, which acts in opposition to the turbine's motion, presenting a resistance that must be overcome for efficient energy extraction. Figure 4 serves as a visual aid, offering a comprehensive depiction of the forces influencing the turbine's performance. A closer examination of this figure reveals that blade number 1 plays a counteractive role, generating a negative torque that resists the turbine's

 https://doi.org/10.1051/e3sconf/202447503002

rotation. In stark contrast, turbine blades 2 and 3 contribute positively to the overall torque, actively enhancing the turbine's rotational motion. The intriguing facet to note is the dynamic relationship between wind velocity and torque production. As wind speeds increase, blades 2 and 3 respond with heightened torque output, bolstering the turbine's efficiency in harnessing wind energy. On the other hand, blade number 1 exhibits an inversely proportional response to wind velocity, leading to reduced torque generation as the wind accelerates. This intricate interplay between forces, torques, and wind velocity highlights the need for a nuanced understanding of the Daeriuss turbine's performance to optimize its energy conversion under diverse environmental conditions. As we can see from Figure 6, the addition of blunt body decreases the wind velocity on the turbine blades. Due to this, the turbine produces negative torque instead of positive and preventing it from rotating back to its original position and generating electricity. The graph of the torque output is shown on Figure 5.

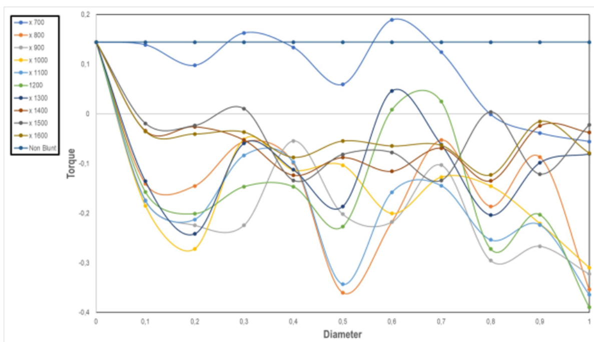

Fig. 5. Torque performance graph.

The graph illustrates that when a blunt body is placed in front of a turbine, it effects the turbine's performance. Most of the time the addition of a blunt body in the front of the turbine will decrease the turbine's torque. This result is consistent with the experiment by Satrio et al, in which the obstacle placed at the 0° position (right in front of the turbine) will decrease the turbine's performance [7]. However, this is not always the case. At a distance of 700 mm and diameter of 0.6 DT, the turbine produces the highest output torque at 0.19 Nm, a slight increase from a non-blunt body turbine at 0.14 Nm. This increase also happens at 700 mm distance and 0.3 DT, which produces torque of 0.16 Nm. This phenomenon happens as there is a small increase in wind velocity of blade number 2 as shown in Figure 6. This increase in the wind velocity happens due to the creation of the wake behind the obstacle and therefore increases the positive torque in the co-rotating zone of the turbine as stated by Zidane et al [8].

Based on the chart, it appears that the blunt body has the greatest impact when positioned between 1000 mm and 1200 mm. Nonetheless, as the distance deviates from this range, the impact gradually diminishes, and the torque regains its strength. Eventually, the torque levels off with that of the non-blunt body, suggesting that the effect of the blunt body has dissipated. Another detail from the chart is every graph produced by each distance is similar. The biggest effect of the blunt body occurs when its diameter is 20%, 50%, and 100% of the diameter of the turbine.

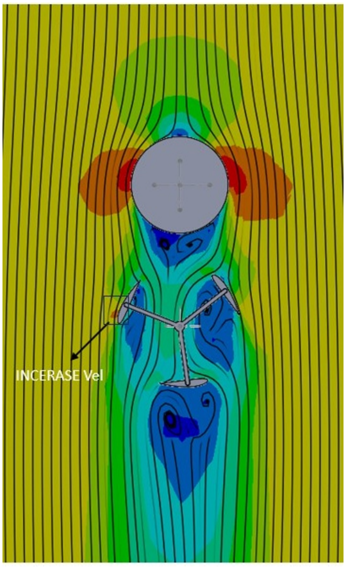

Fig. 6. Velocity contour plot of the simulation.

As we move past 700 mm distance, the effect that the blunt body has on the turbine will cause the torque value to lower even more. The lowest produced torque value is at 1200 mm distance and 1 DT which produced a torque of -0.39 Nm. Past 1200 mm however, the decrease in torque is not as severe. According to the obtained data, it is recommended to place the turbine 1.6 meter or further to minimize the decreasing torque. However, if the distance between the obstacles is less than 1.6 meter, it is advisable to ensure that the turbine is positioned at a minimum distance of 0.7 meters from any obstacles that are less than 1.6 meters in proximity, and that the turbine diameter is 67% larger than the diameter of the obstacle.

4 Conclusions

From the simulation performed, it was found that light poles will effect the torque produced by the turbine. The effect depends on the x-axis distance of the pole from the turbine and the pole diameter. Generally, the placement of the light poles will decrease the torque of the turbine. This is due the decreased wind velocity around the turbine blades caused by the blunt body. The safest placement distance of the turbine is 700 mm in the x-axis from the blunt body with blunt body diameter of 0.6 DT or 0.3 DT as it can increase the turbine's torque output albeit not much. These results indicate that the placement of the turbine in relation of other objects, such as light poles, needed to be taken into account such that it will not impair the turbine's performance.

References

1. Directorate of Distribution Statistics, *Land Transportation Statistics 2021* (BPS RI, Jakarta, 2022)
2. E.H. Bani-Hani, A. Sedaghat, M. Al-Shemmary, A. Hussain, A. Alshaieb, H. Kakoli, Ener. Eng. **115**, 61-74 (2018)
3. S.A.H. Nassir, F.M. Zawawi, M.Z. Mazlan, S. Samion, M.A.W.M. Yazid, U. Abidin, J. Adv. Res. Fl. Mech. Th. Sci. **57**, 175-184 (2019)

https://doi.org/10.1051/e3sconf/202447503002

4. T. Hidayat, *Wind Power in Indonesia: Potential, Challenges, and Current Technology Overview,* in Indonesia post-pandemic outlook, 109-132 (2022)
5. K.M. Saqr, M.N. Musa, J. Ener. Pol. **39**, 3873-3877 (2011)
6. A. Sobachkin, G. Dumnov, *Numerical Basis of CAD-Embedded CFD*, In Proceedings of the NAFEMS World Congress, NWC13, 9-12 June 2013, Salzburg, Austria (2013)
7. D. Satrio, Suntoyo, F. Albatinusa, S. Junianto, S. Musabikha, Madi, F.O. Setiawan, *Effect of Positioning a Circular Flow Disturbance in Front of the Darrieus Turbine*, In Proceedings of the The 7th International Conference on Marine Technology, SENTA 2022, 20 October 2022, Surabaya, Indonesia (2022)
8. I.F. Zidane, H.M. Ali, G. Swadener, Y.A. Eldrainy, A.I. Shehata, Alexandria Eng. J. **63**, 175-189 (2023)